How does negative triangularity mitigate ITG turbulence and transport?

[Under review NF 2024]

Rameswar Singh, P H Diamond and A Marinoni
UCSD

66^{th} APS DPP, Atlanta, October 11, 2024

Acknowledgements: G Merlo & U.S. Department of Energy Award Number DE-FG02-04ER54738.

Motivation

- Improved confinement in NT over PT tokamak experiments is now well established. [Y Camenen+ 2007, M Fontana+2018, M Austin+ 2019, A Marinoni+ 2019, S Coda+2022,…]

- Theoretical understanding lacking! TEM/ITG stabilization often invoked to explain improved confinement in NT.
  - TEM stabilization by precession drift reduction. [A Marinoni+ 2009]
  - ITG turbulence and transport for NT remains poorly understood.

- Previous simulations lacked insights on physical mechanism behind the beneficial effects of NT on ITG . Sometimes, not even general agreement on basic trends with δ!

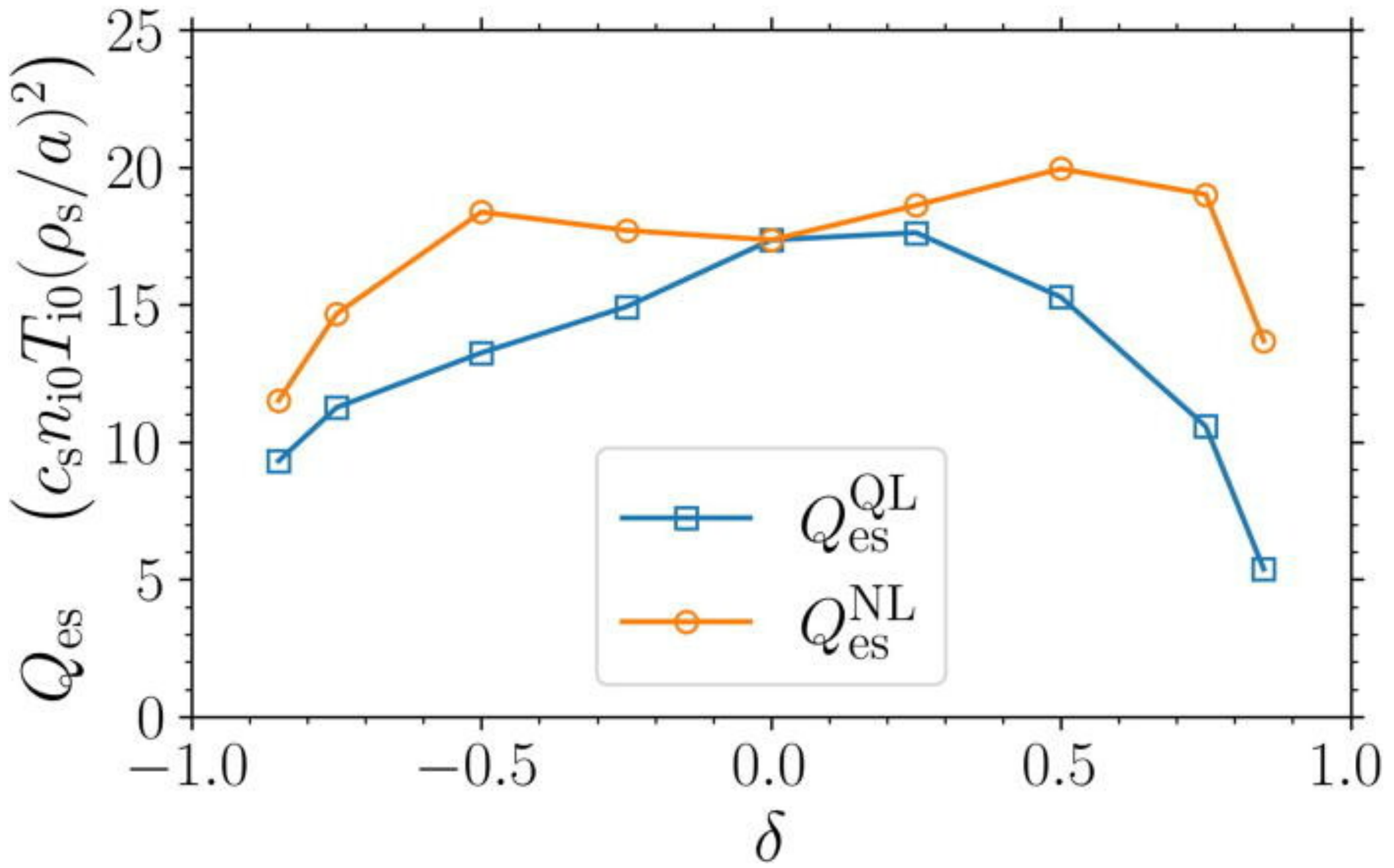

[J M Duff+ 2022]

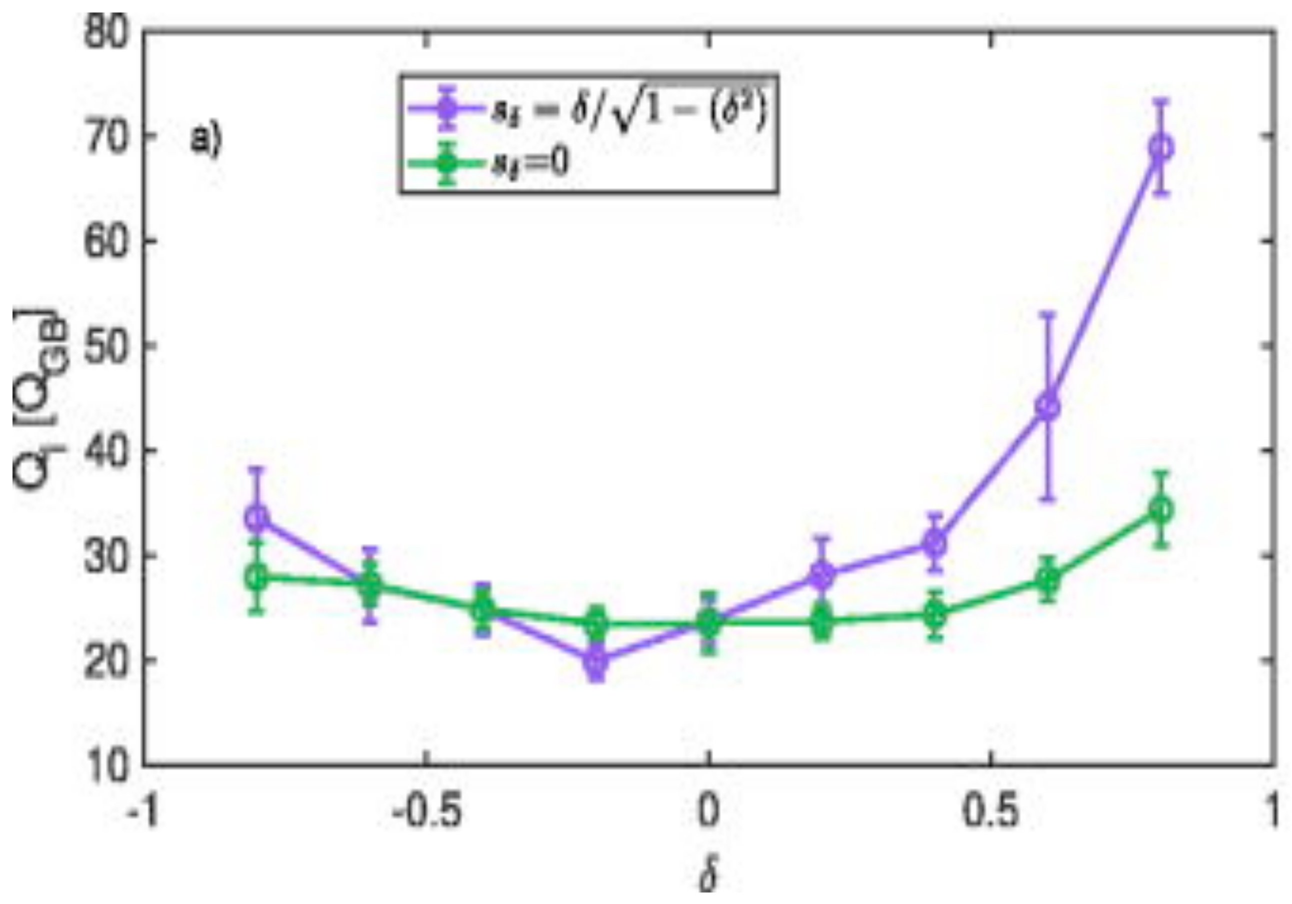

[G Merlo+ 2023]

Questions remain…

- What causes the reduced linear growth rate for NT?
- What explains the δ-trend of heat flux?
  - Relative role of fluctuations amplitude and cross-phase in determining the heat flux for NT?
  - Saturation by zonal flows well known in GK simulations [Z Lin+ 1998,1999,…others]. What happens to self-generated zonal flow shear for NT?

Simulation set up

- **Disclaimer:** This is a physics study, not an experimental validation exercise.

- GENE flux tube simulations of collisionless ITG turbulence with adiabatic electrons. Profiles fixed, triangularity varied.

- **Shaping parameters:** aspect ratio $a/R = 1/3$, safety factor $q = 2$, magnetic shear $\hat{s} = 1$, triangularity $\delta = [varied]$, triangularity gradient $S_\delta = \frac{r\frac{\partial\delta}{\partial r}}{\sqrt{(1-\delta^2)}} = \frac{\delta}{\sqrt{(1-\delta^2)}}$, elongation $\kappa = 1$, elongation gradient $S_\kappa = \frac{r}{\kappa}\frac{\partial\kappa}{\partial r} = 0$, squareness $\zeta = 0$, squareness gradient $S_\zeta = r\frac{\partial\zeta}{\partial r} = 0$, MHD alpha parameter $\alpha_{MHD} = -q^2 R\frac{d\beta}{dr} = 0$, Shafranov shift gradient $R_0' = 0$. (Standard GA + shaping)

- **Resolutions:** $n_x = 257$, $n_{k_y} = 48$, $n_z = 64$, $n_{v_\parallel} = 48$, $n_\mu = 8$, $L_{v_\parallel} = 3$, $L_\mu = 9$, $L_x = [120 - 140]\rho_i$, $k_{y,min}\rho_i = 0.05$, hyp_z=2, hyp_v=0.2

- **Gradients:** $a/L_n = 1$, $a/L_T = 4$ [fixed]
- **Collisionless:=> no frictional damping of ZF.**
- **No neoclassical transport.**

Linear growth rates are reduced for NT

- Growth rates are lower for NT than for PT.

- **Why?**
- **Linear stability linked to eigenmode averaged quantities $\langle \omega_{Dy} \rangle, \langle k_\perp^2 \rangle, \langle k_\parallel^2 \rangle$.**

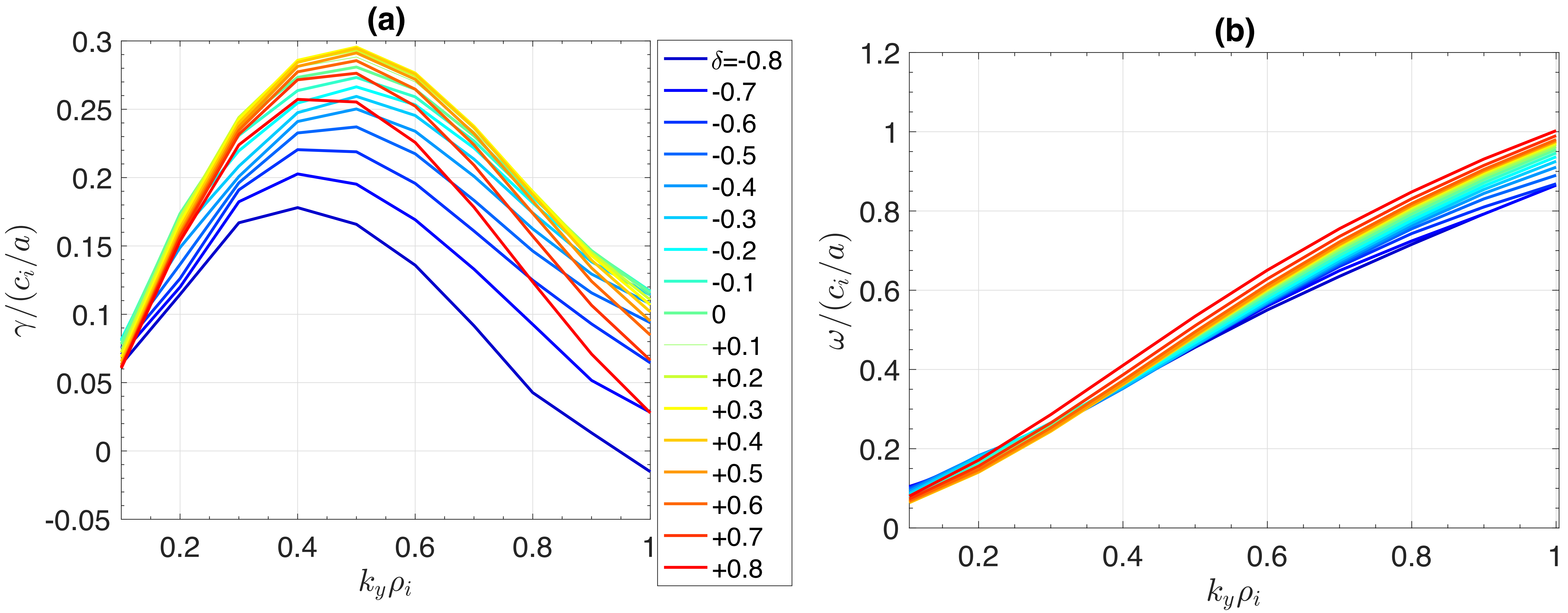

Eigenmode averaged magnetic drift frequency is reduced for NT

- Eigenmode averaged drift frequency:

$$\left\langle \omega_{Dy} \right\rangle = \frac{\int d\theta JB |\phi|^2 \omega_{Dy}}{\int d\theta JB |\phi|^2}, \text{ where}$$

  - $\omega_{Dy} = k_y \frac{v_\parallel^2 + v_\perp^2/2}{\Omega} \mathscr{K}_y$ is binormal magnetic drift frequency
  - $\mathscr{K}_y = \frac{1}{B} \vec{b} \times \vec{\nabla} B \cdot \vec{\nabla} y$ is binormal curvature

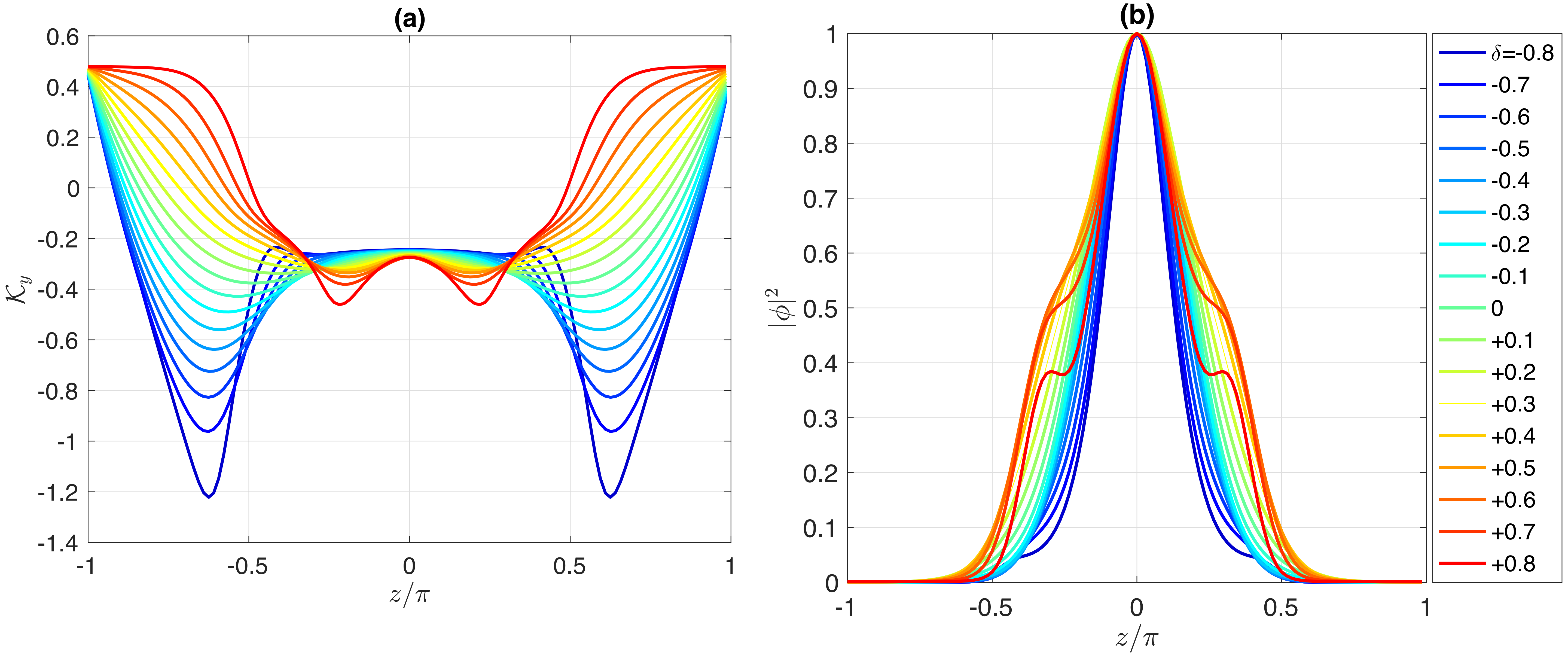

- $\mathscr{K}_y$ less negative for at $z = 0$ NT.
- Broader negative $\mathscr{K}_y$ region for NT.
- But thinner eigenmode width for NT

➡Less negative $\left\langle \omega_{Dy} \right\rangle$ for NT. →

➡**weaker effective curvature drive for NT, due to reduced sampling of the bad curvature regions resulting from a narrow eigenmode structure in NT.**

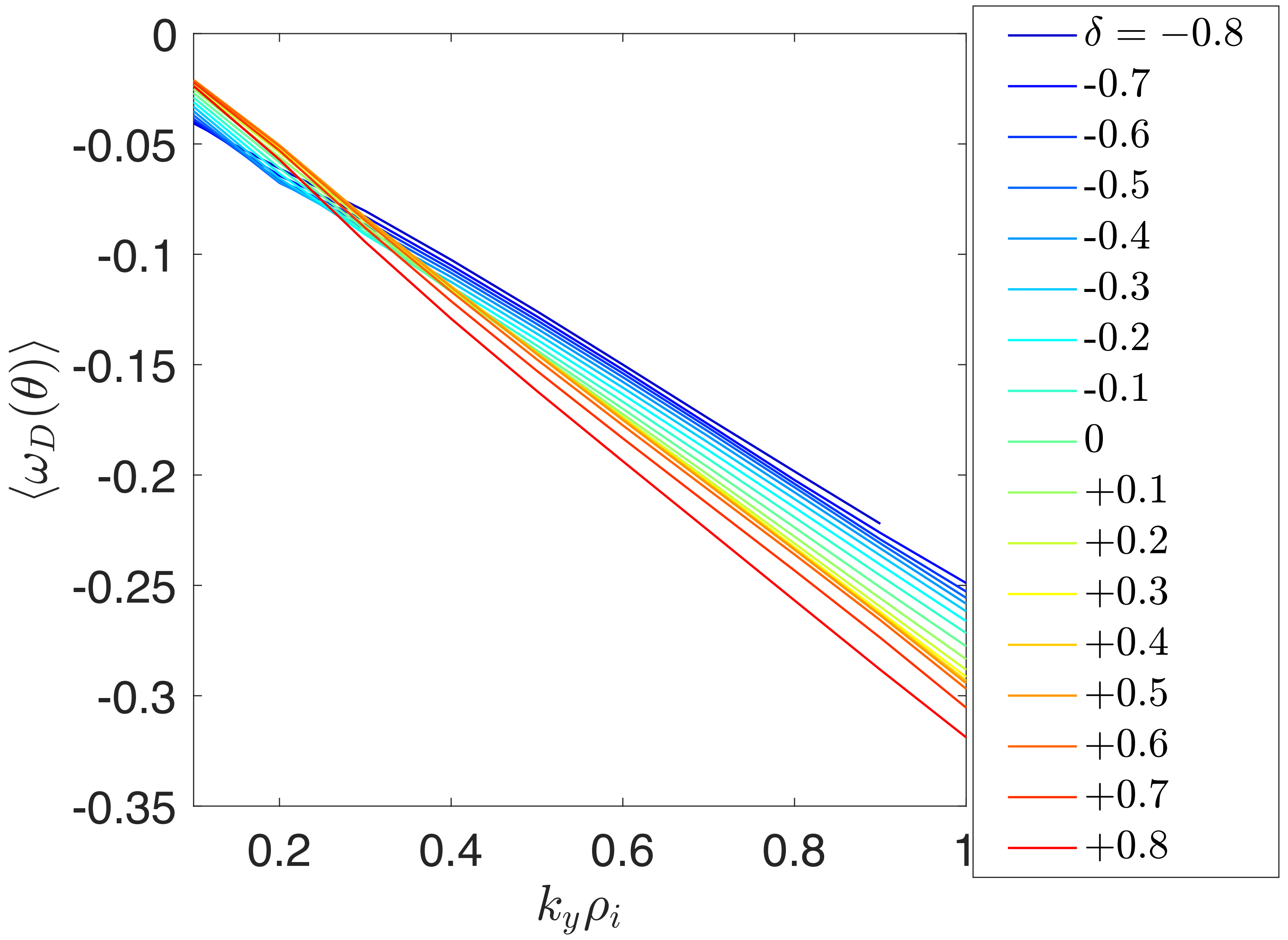

Local magnetic shear $\tilde{s}$

- $\tilde{s} = \dfrac{r}{\nu}\dfrac{\partial \nu}{\partial r}$, where $\nu = IJ/R^2$ is the local safety factor.

- More and more negative $\tilde{s}$ in the bad curvature region and the poloidal extent of the $\tilde{s}$<0 region expands for stronger NT shapes

- **→easier to twist eddies towards the good curvature side as you move along the field line →better stability for NT!**

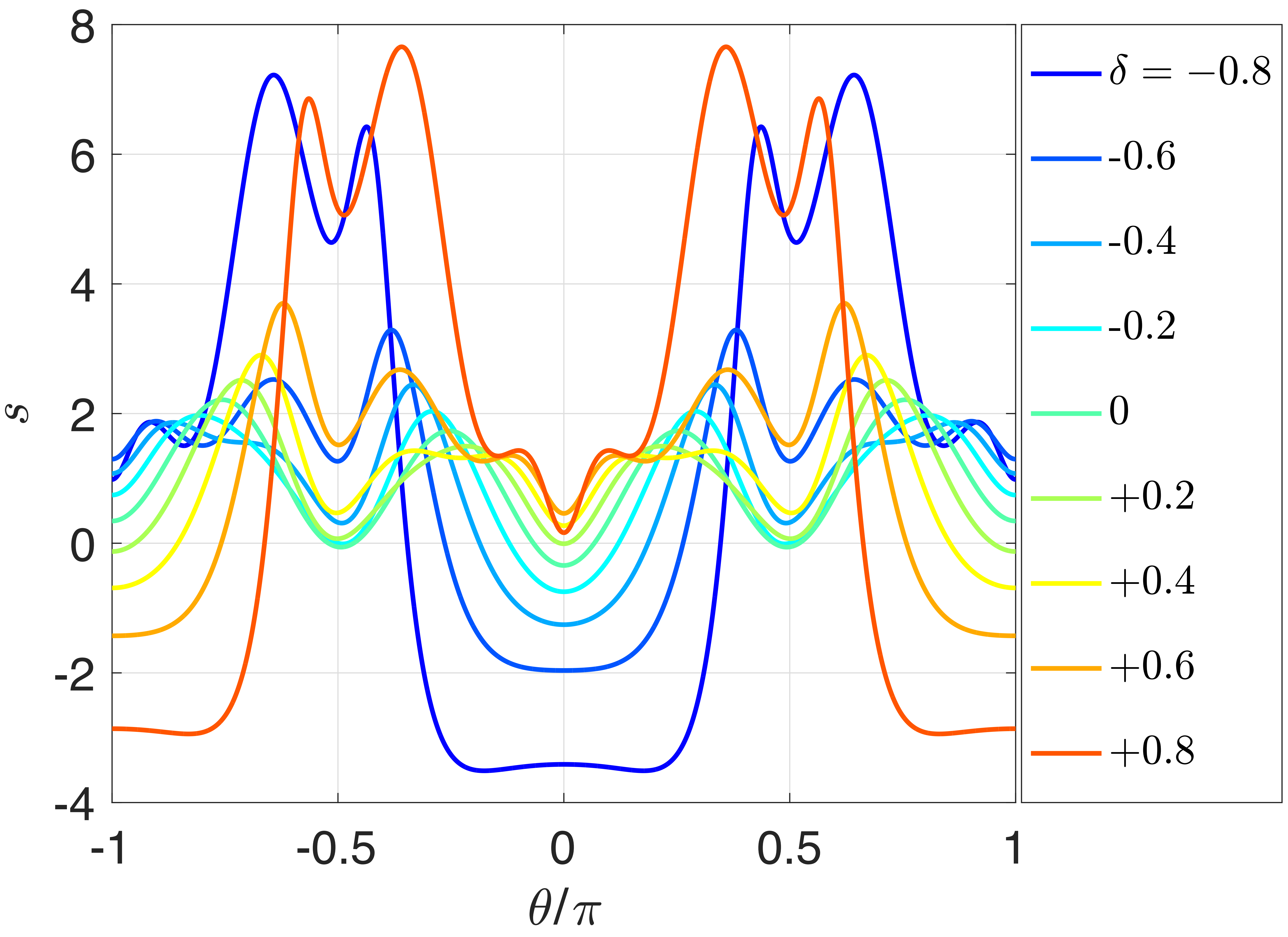

Nonlinear Heat flux vs Triangularity

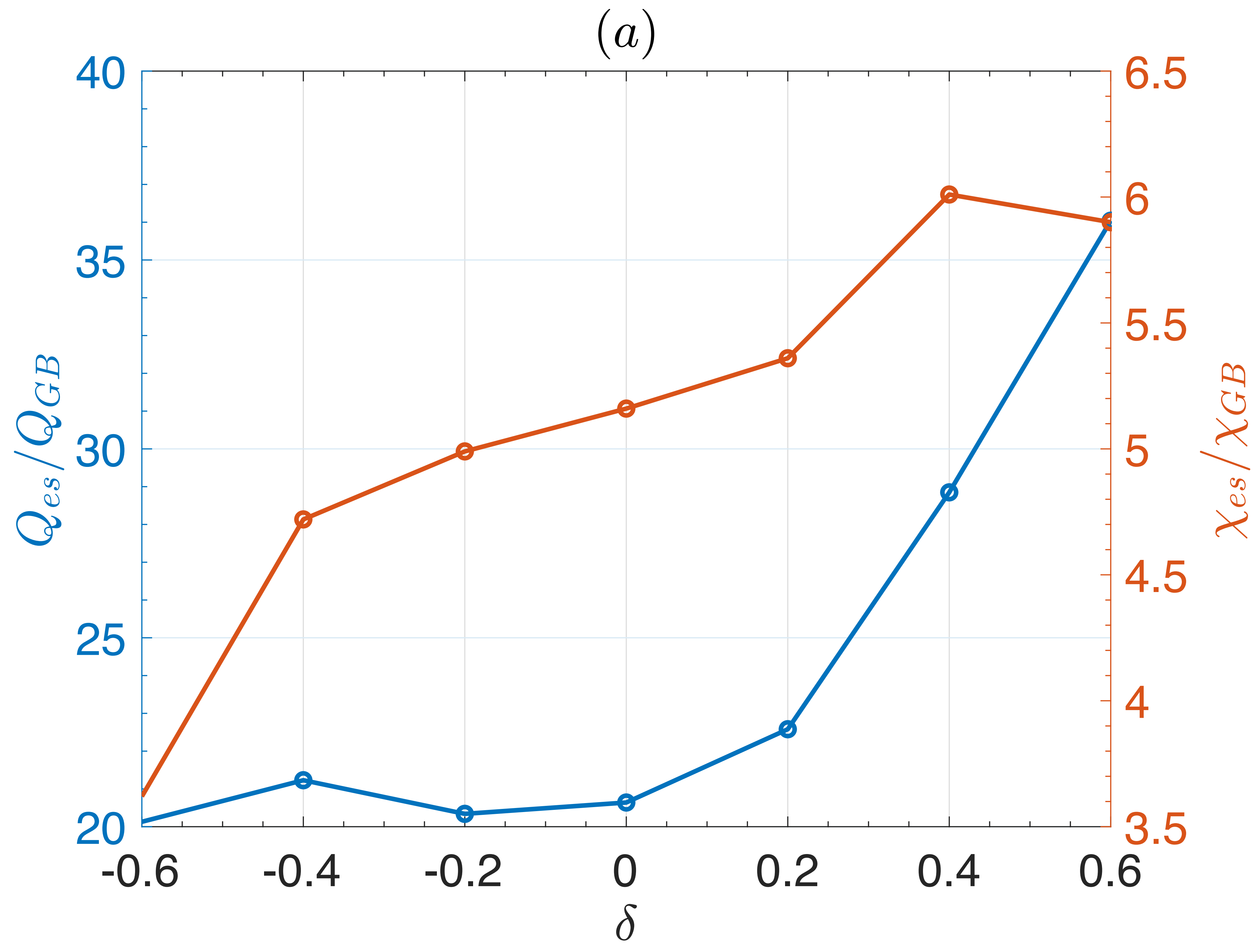

- Heat flux $Q_i = \left\langle \sum_{\vec{k}} -k_y \left| T_k \right| \left| \phi_k \right| \sin(\theta_T - \theta_\phi) \right\rangle$

Amplitudes **Cross-phase**

- Turbulent heat diffusivity lower for NT than for PT.

- High k_y contributions (RHS of the spectral peak) depleted more for NT.

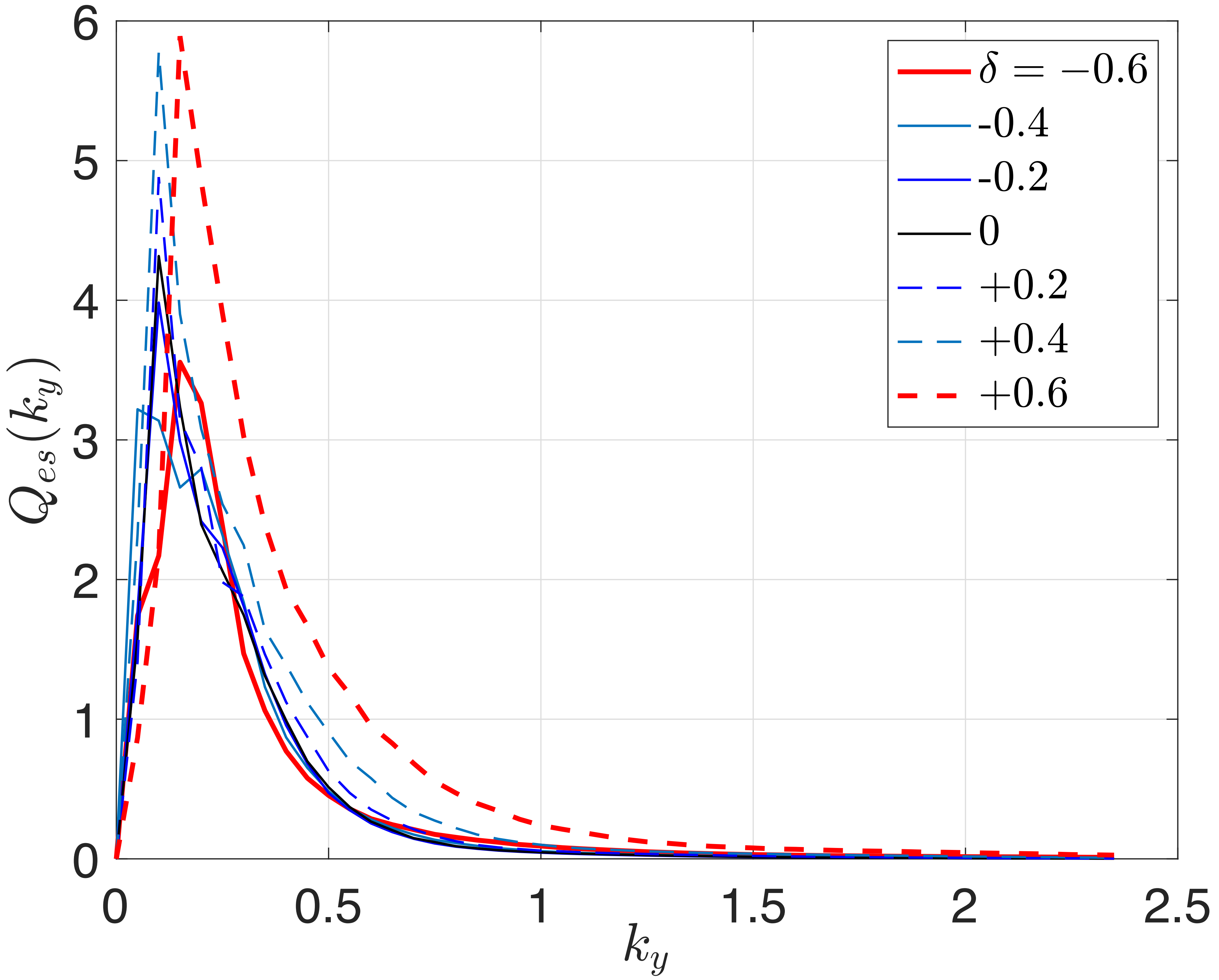

Saturated fluctuation intensity vs Triangularity

- Fluctuation intensities are lower for NT than for PT.
- Fluctuation kinetic energy: $FKE = \left\langle \sum_{k_x,k_y} \left[1 - \Gamma_{0i}(k_\perp^2 \rho_i^2)\right] \left| \frac{e\delta\phi_k}{T_i \rho^\star} \right|^2 \right\rangle$ is lower for NT!

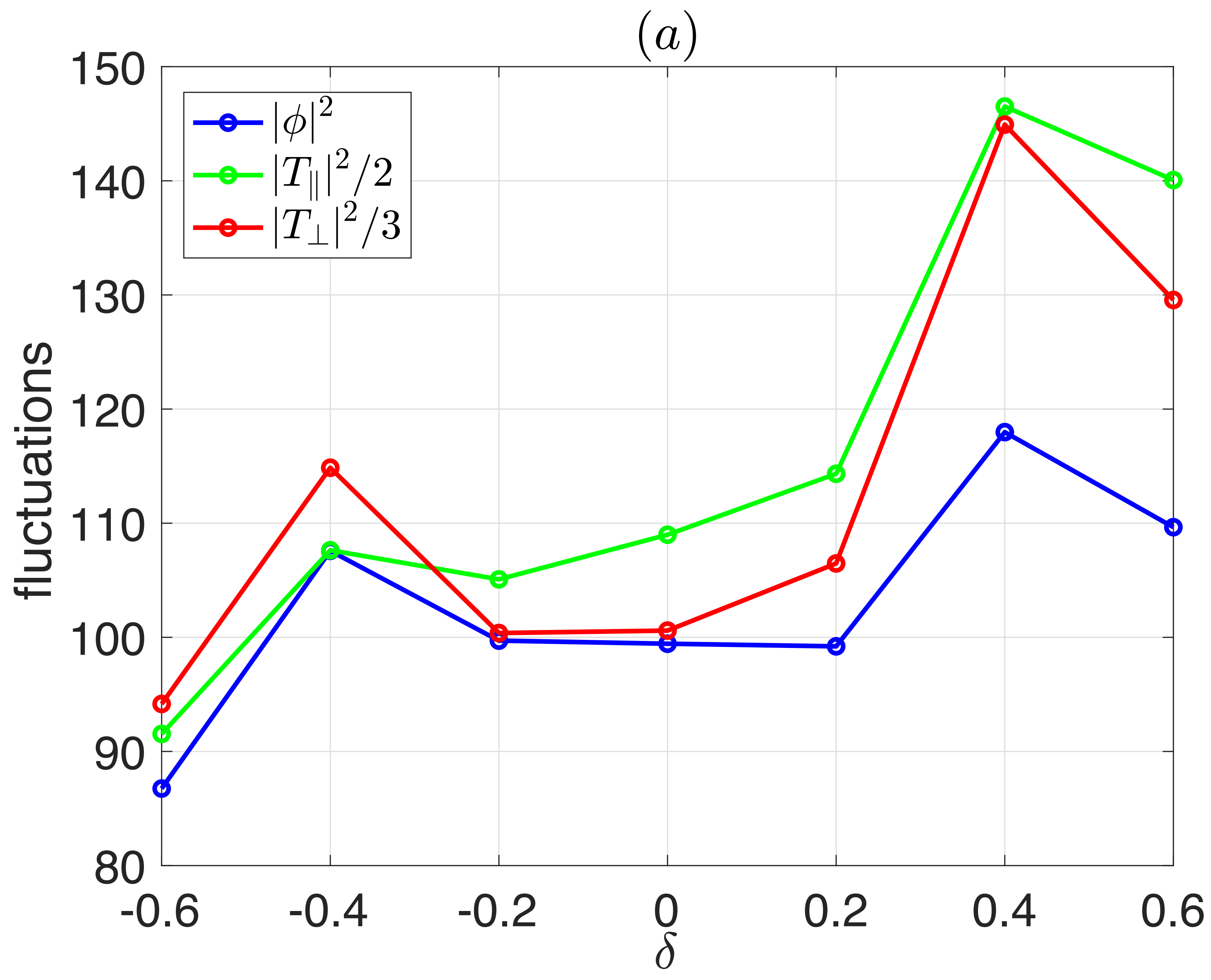

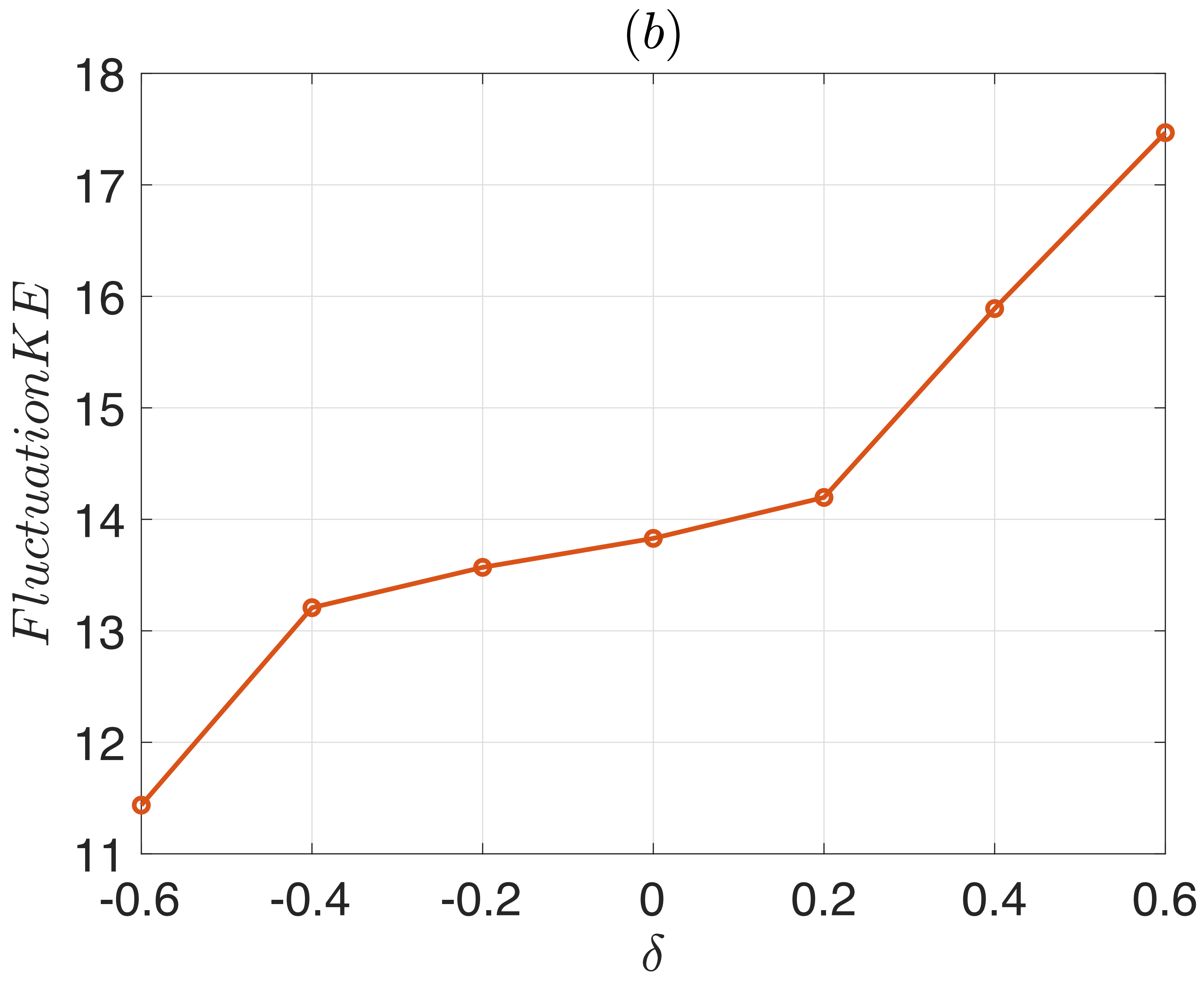

Transport cross-phase spectra vs Triangularity

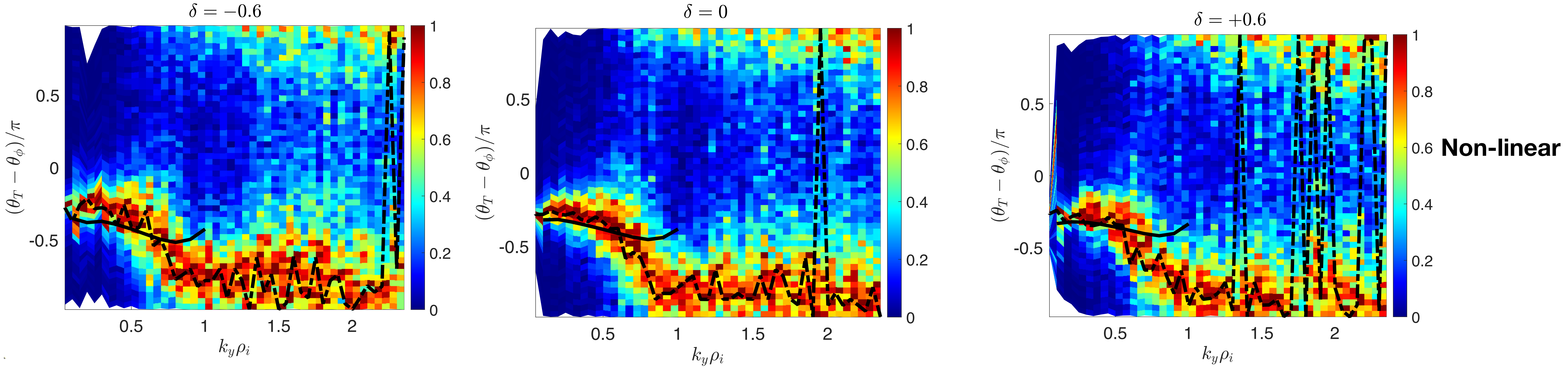

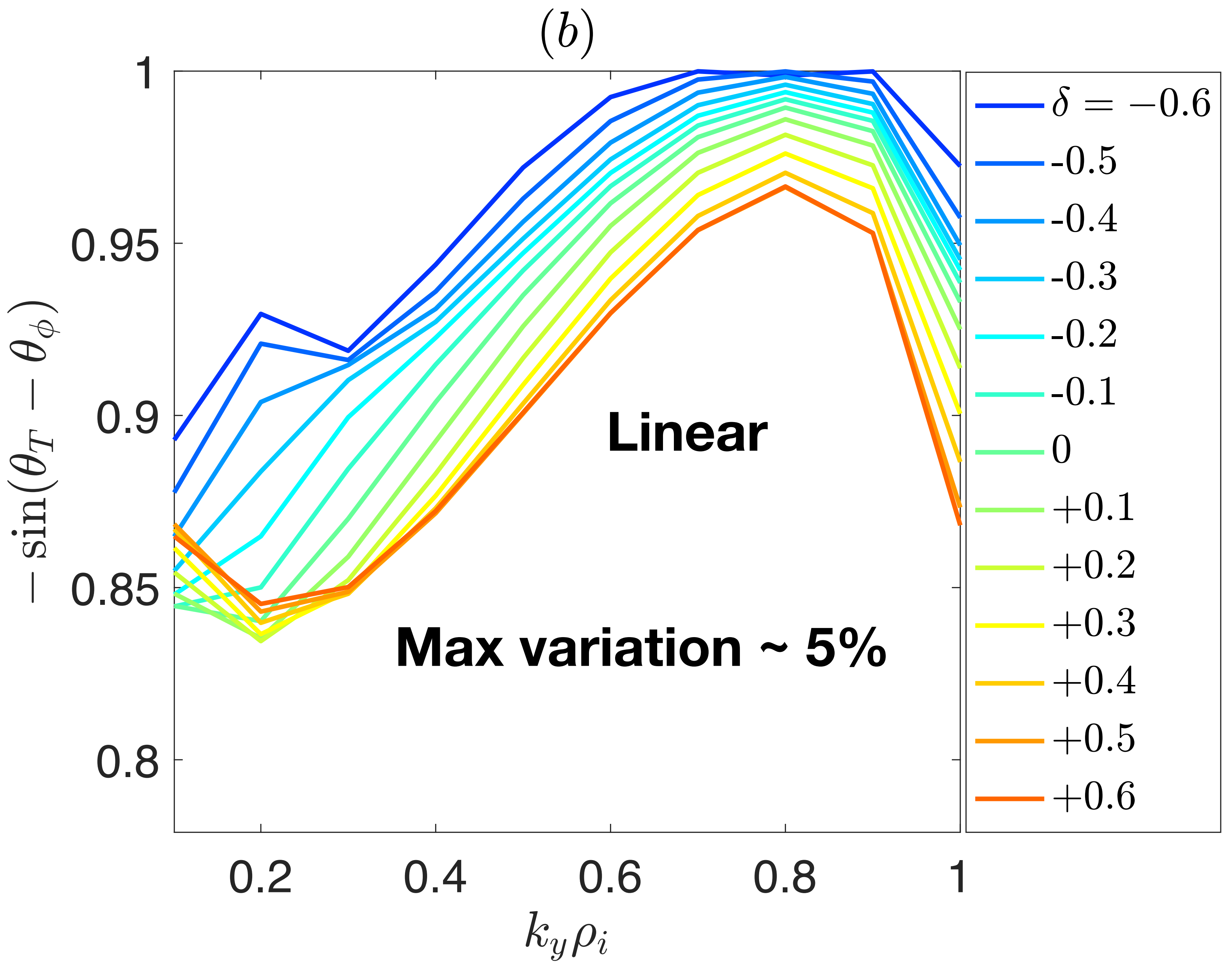

- Cross phases between temperature and potential fluctuations $(\theta_T - \theta_\phi)$ are weakly sensitive to δ.

➡**Transport reduction for NT is pre-dominantly due to reduction of fluctuation amplitudes.**

Fluctuations auto-correlation and random walk diffusivity

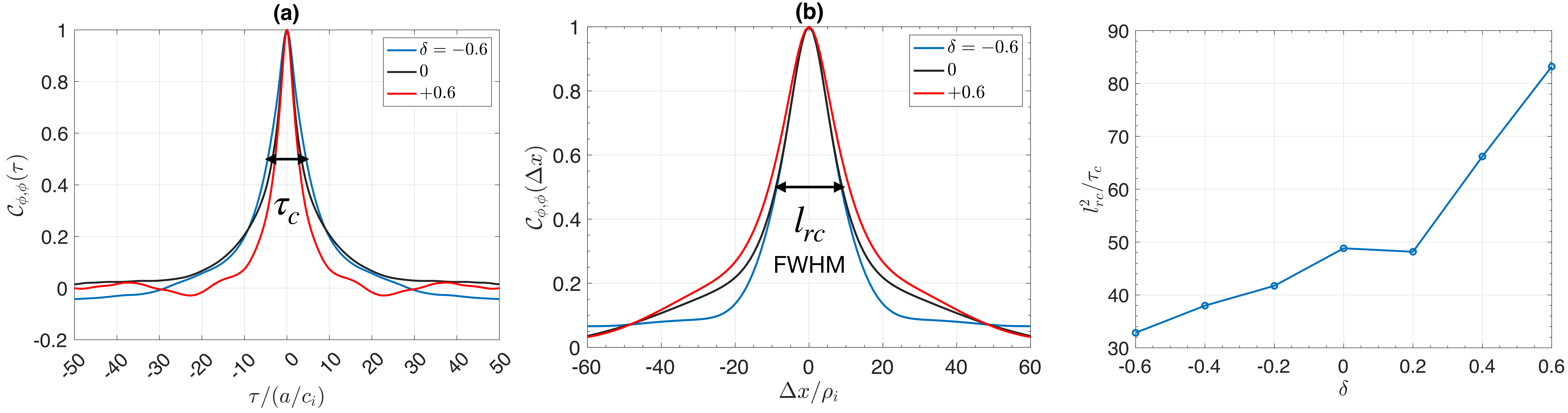

- Auto-correlation time higher for NT: $\tau_c(NT) > \tau_c(PT)$
- Radial auto-correlation length lower for NT: $l_{rc}(NT) < l_{rc}(PT)$ [Consistent with TCV experiment: M Fontana+ 2018]

➡ Random walk diffusivity $\frac{l_{rc}^2}{\tau_c}$ lower for NT.

Zonal ExB shearing rates: $\omega - k$ spectra

- Shearing spectra are highly sensitive to δ.
    - No dispersive effect for $\delta = -0.6$
    - Clear dispersive effects for $\delta = 0$→propagating zonal flows (New branch)
    - Weak dispersion for $\delta = +0.6$
- The spectra roll over at ~GAM frequency

Zonal ExB shearing rates: spatiotemporal features

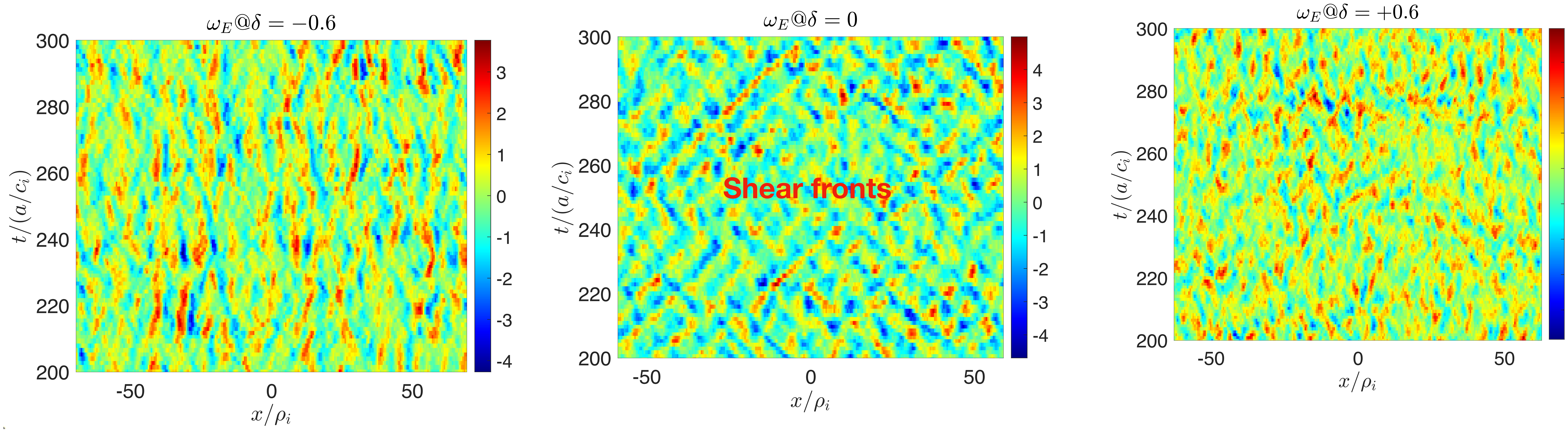

- Spatiotemporal patterns are highly sensitive to δ.
  - **Spatiotemporal shearing pattern more coherent for NT than for PT.**
  - Propagating shearing fronts → dispersive feature for $\delta = 0$! Front speed $\sim 2.25\rho_\star v_{th}$.
- **More coherent spatiotemporal shearing pattern for NT → Stronger mean shearing effect for NT.**

RMS Zonal ExB shearing rates at saturated state

- **Zero-frequency RMS shearing rate higher for NT than for PT.**
- Total RMS shearing rate and finite frequency RMS shearing rate decreases with increasing $|\delta|$.

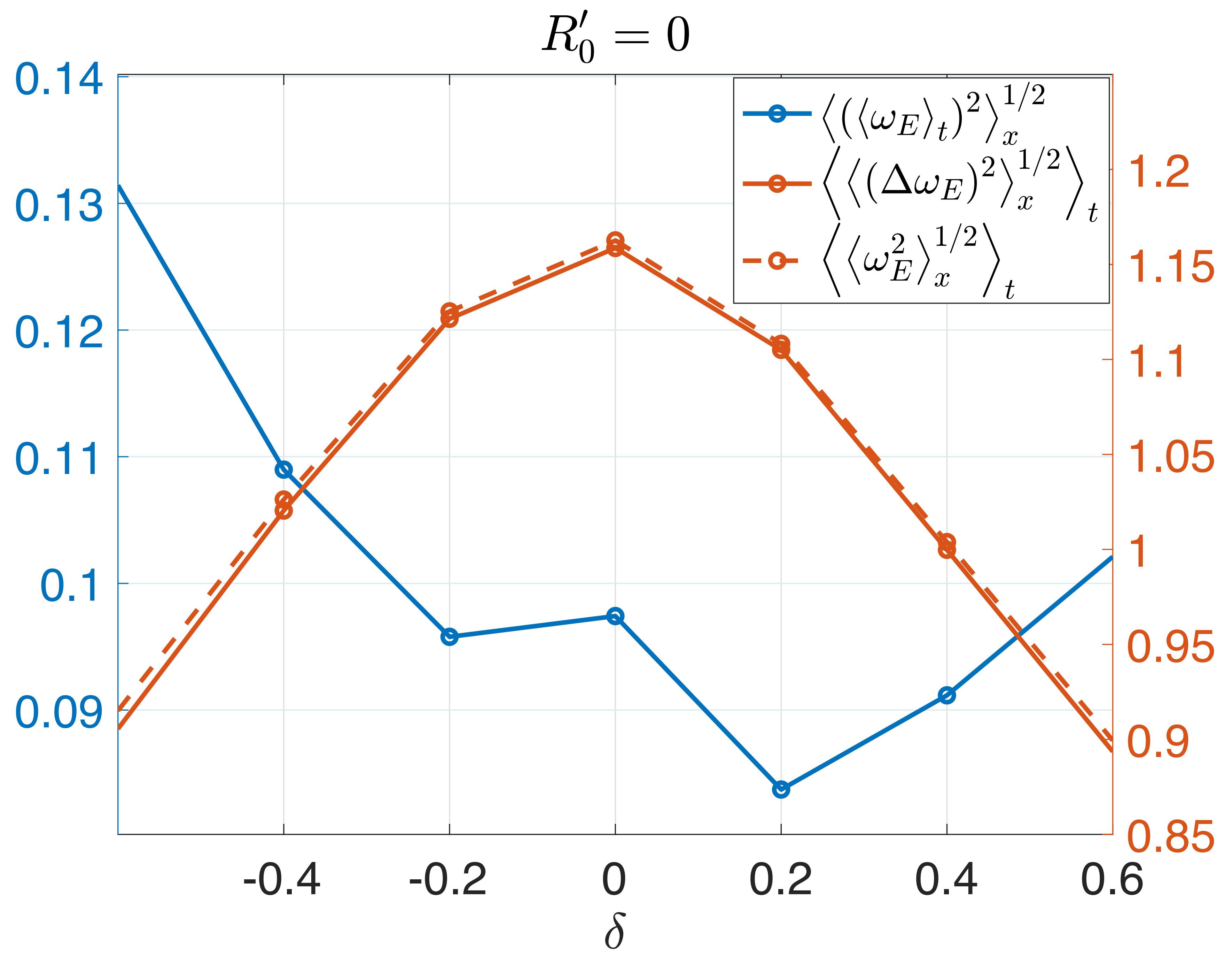

✳ Time averaged or zero-frequency RMS shearing rate: $\left\langle \left\langle \omega_E \right\rangle_t^2 \right\rangle_x^{1/2} = \left[\frac{1}{L_x} \int dx \left\langle \omega_E(x,t) \right\rangle_t^2 \right]^{1/2}$, where $\left\langle \omega_E(x,t) \right\rangle_t = \frac{1}{T} \int dt \omega_E(x,t)$

✳ Total RMS shearing rate : $\left\langle \left\langle \omega_E^2(x,t) \right\rangle_x \right\rangle_t^{1/2} = \left[\frac{1}{T} \int dt \frac{1}{L_x} \int dx \omega_E^2(x,t) \right]^{1/2}$

✳ Standard deviation of shearing rate: $\left\langle \left\langle \left(\Delta\omega_E \right)^2 \right\rangle_x^{1/2} \right\rangle_t = \left\langle \left\langle \left(\omega_E(x,t) - \left\langle \omega_E(x,t) \right\rangle_t \right)^2 \right\rangle_x^{1/2} \right\rangle_t$

RMS shearing rate depends on the detail of the shearing spectra at saturated state

- **Different δ-trend of zero-frequency shearing rate and zonal potential spectra.**
- Zonal shear peak at $k_x\rho_i \sim 0.5$ whereas zonal potential peak at $k_x\rho_i \sim 0.05$.
- **Shearing peak stronger while potential peak weaker for NT.**

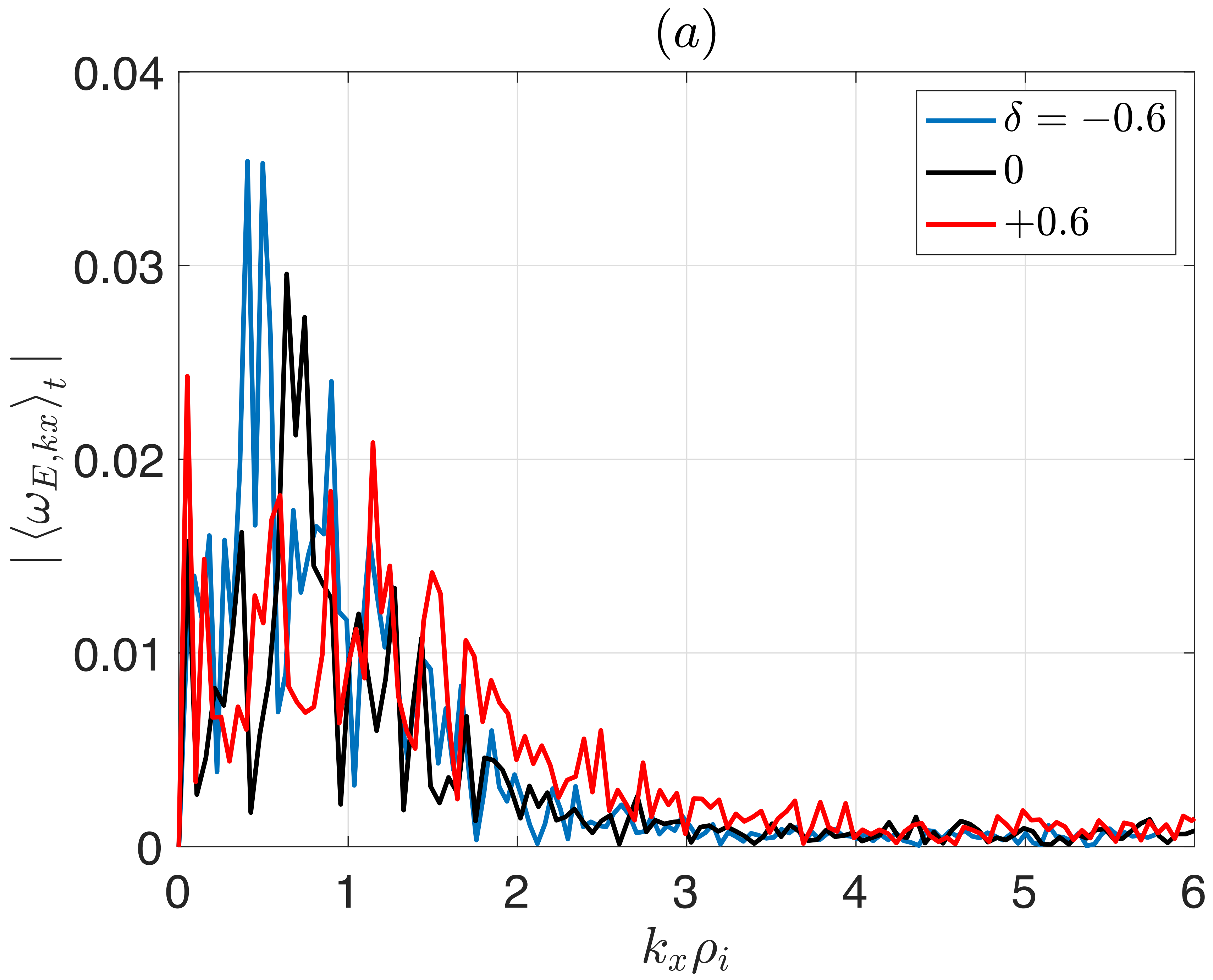

Shearing peaks stronger for NT than for PT.

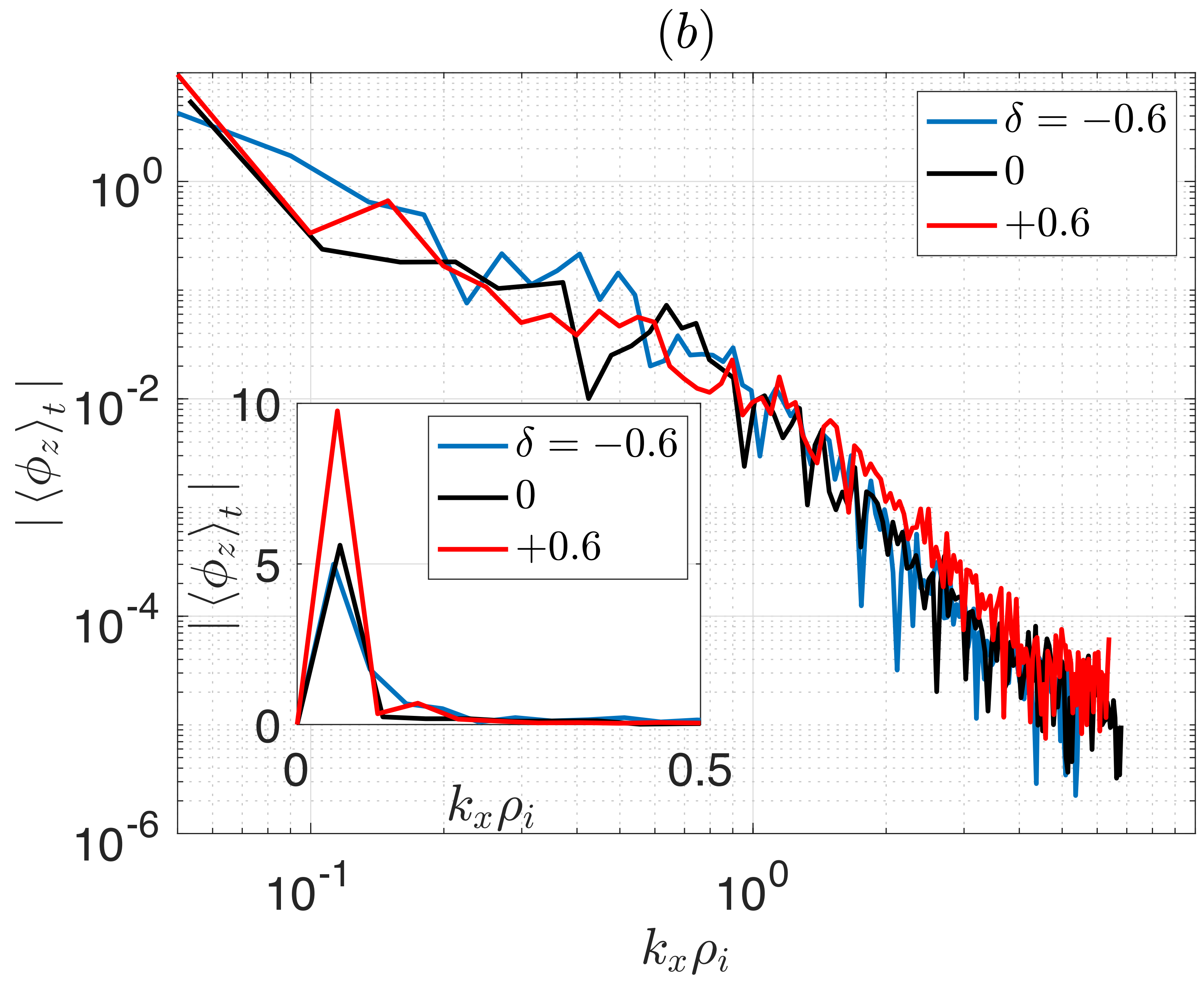

Zonal potential peaks weaker for NT for PT. But zonal potential isn't the point.

Figure of Merit

- All analyses point at the dimensionless parameter $\omega_E\tau_c$ or ω_E/γ_{max} as *figure of merit*.

- $\omega_E\tau_c$ higher for NT than for PT. Nicely correlates with the δ-trend of heat diffusivity.

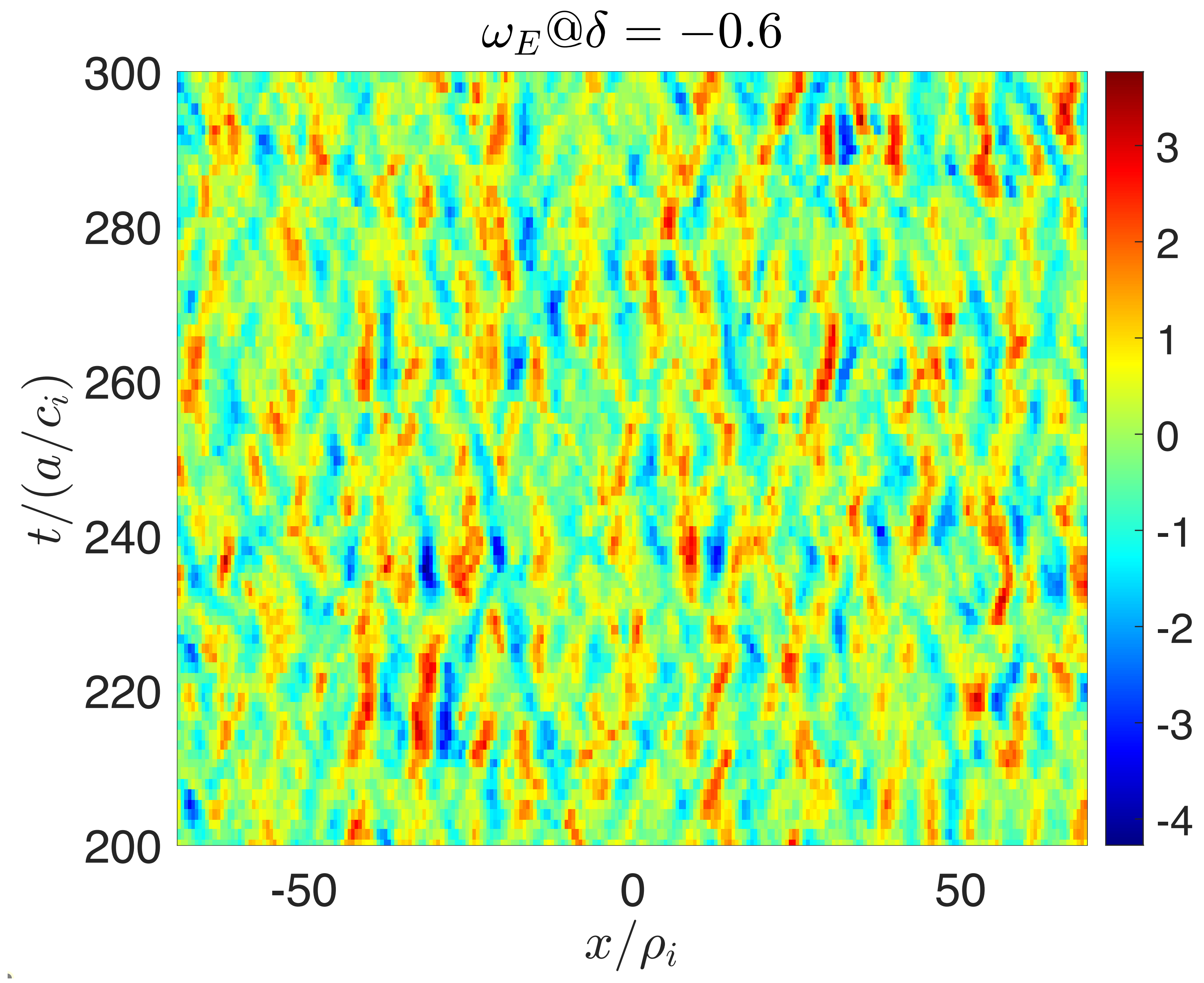

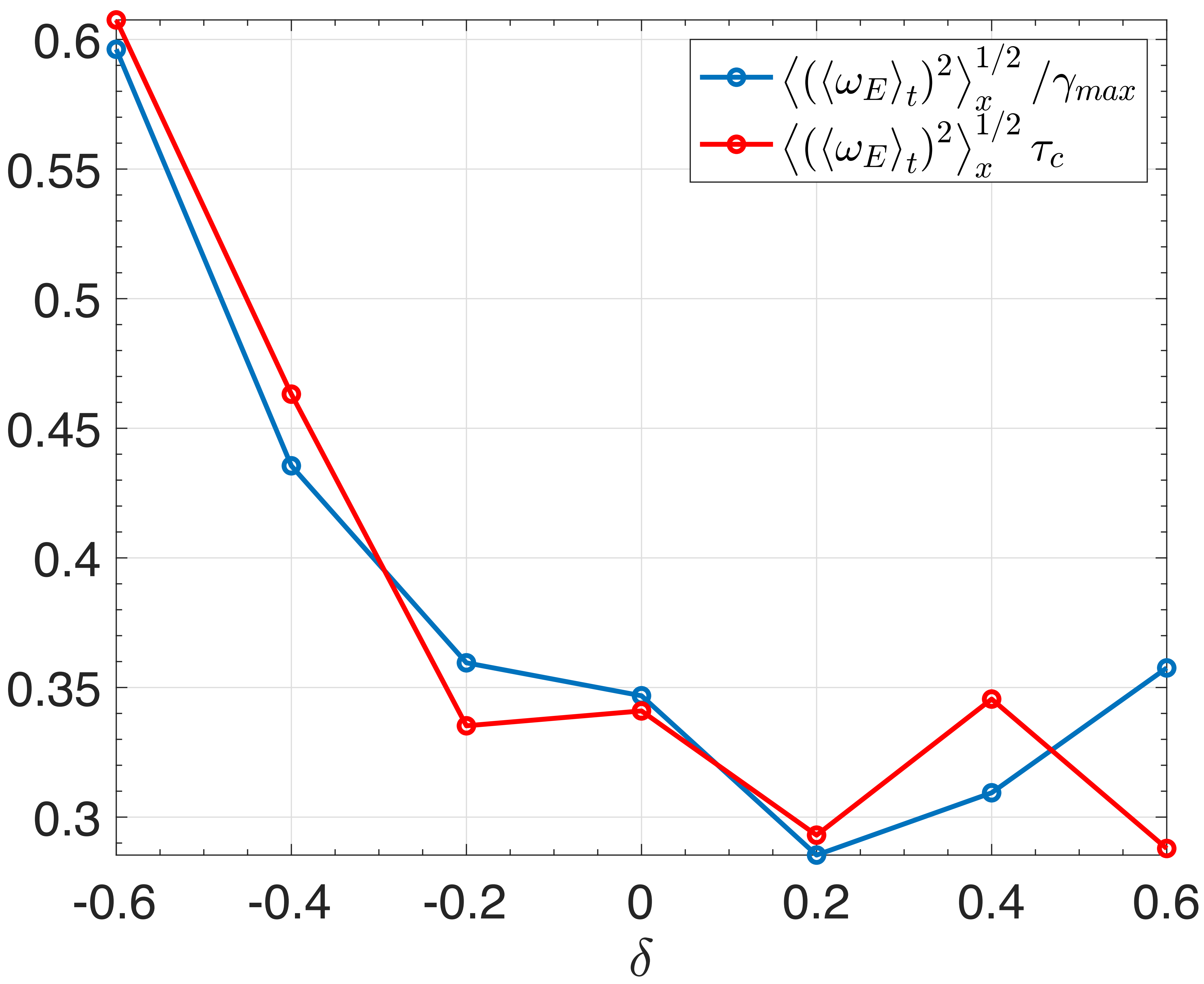

Summary

- Novel insights into how NT mitigates ITG turbulence and transport
  ↓
  $\omega_E \tau_c$ or ω_E/γ_{max} as *figure of merit.*

- Reduced linear growth rate for NT
  ↕
  Reduced eigenmode averaged magnetic drift frequency.

- Reduced heat flux for NT
  ↕
  Reduced radial correlation length and increased correlation time due to increased zero-frequency zonal ExB shearing rate.

- δ-trend of diffusivity
  ↓
  Predominantly determined by δ-trend of fluctuation amplitude. Cross-phase effect weak.

Future work

- Understanding why zero-frequency zonal shearing stronger for NT →requires analysis of Reynolds power $\frac{\partial \langle v_\theta \rangle}{\partial r} \langle \tilde{v}_r \tilde{v}_\theta \rangle$. More generally, gyrokinetic nonlinear entropy transfer analysis required. Collisionless zonal flow saturation dynamics?

- Analysis using experimental equilibria and profiles and using non-adiabatic electrons and finite collisionality exploiting both local and flux driven global simulations.

For experiments

- **Measure $\omega - k$ spectra of the zonal flow shear**. Identify finite frequency components? Spatio-temporal features of zonal shear, signatures of propagating zonal fronts→BES velocimetry
- Study, identify different trends of zero-frequency zonal potential and zonal flow shear with δ.
- Bi-spectral analysis to identify how dominant interactions change with triangularity ?
- Frequency resolved Reynolds power $\frac{\partial \langle v_\theta \rangle}{\partial r} \langle \tilde{v}_r \tilde{v}_\theta \rangle$ vs triangularity to elucidate turbulence—> zonal flow energy coupling? →BES velocimetry.
- Radial correlation length and auto-correlation time of fluctuations and zonal flows. **Calculate FOM $\omega_E \tau_c$ vs δ.**

Back-up slides

Heat flux avalanches

- Avalanches also seen in heat flux space time evolutions.

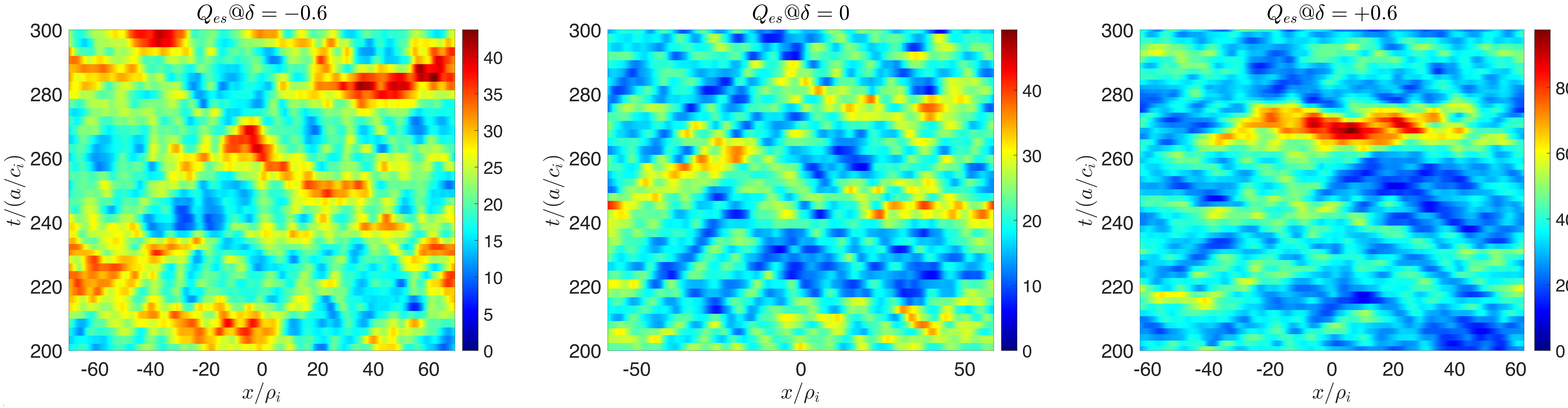

Temperature corrugations dynamics

(a) Zonal temperature spectrally anti-correlated with zonal potential $T_{z,k_x} \propto -\phi_{z,k_x}$. Consequently, zonal ExB shear ω_E is spatially anti-correlated with zonal temperature curvature $\nabla^2 T_z$.

(b) Zonal temperature corrugations are stronger for NT than for PT.